



Relaxation of the weak scale

Llibert Aresté Saló,

Universitat Politècnica de Catalunya (Barcelona).

Susan van der Woude,

Rijksuniversiteit Groningen.

Supervised by:

Christophe Grojean,

DESY-Theory Group (Hamburg).

September 7, 2016

Abstract

In this report, we are going to discuss a new solution to the electroweak hierarchy problem called Relaxation. We will introduce a scalar axion-field that screens the value of the Higgs vacuum expectation value (vev). Thus, we will show that this mechanism could result in a small Higgs vev at the end of the dynamical evolution. Finally, we are going to talk about superradiance around spinning black holes and its connection to axions.

Contents

1	Introduction	3
2	Hierarchy problem	4
3	Relaxation model	6
4	Double scanner mechanism	10
5	Superradiance	18
5.1	Kerr Black Holes	19
5.2	Superradiance condition	20
5.3	Distribution of black holes	23
6	Conclusions	26
7	Acknowledgements	26

1 Introduction

The mass of the Higgs particle (125 GeV) is not stable under radiative corrections from Beyond Standard Model (BSM) states with large masses ¹. Extreme fine-tuning is needed to cancel these radiative corrections and obtain a small physical Higgs mass. This is called the Hierarchy problem. The two standard approaches to solve the Hierarchy problem are supersymmetry and composite Higgs models. But both have not been verified by experiments at for example the LHC. In this report, we are going to talk about a new approach to solve the Hierarchy problem, called Relaxation [3].

The Relaxion model [3] considers a potential which takes into account the interaction between a scalar axion-like field, ϕ , (called the relaxion) and the Higgs field. This Higgs-axion term in the potential results in bumps in the potential when the Higgs vev is non-zero. The scalar field starts from a high enough initial value so that the Higgs vacuum expectation value is zero. Then it rolls down until reaching a critical value ϕ_c , where Higgs vev and the bumps start to grow. With the aid of the Hubble friction, the field gets trapped in a potential minimum, which is rather close to the critical value, thus reaching a vev that is much smaller than the cut-off of the model.

The report is organised as follows: first the Hierarchy problem and how it arises in BSM theories will be explained in some detail. After that, some simulations of the Relaxion model will be shown and constraints on these models will be discussed. Then, we are going to study, as well, the relaxation model after the introduction of yet another axion field [4]. Finally, we are going to treat superradiance around spinning black holes, which can offer us a possible way to detect axions.

¹This is a general feature of all scalar particles: unlike gauge bosons and fermions the mass of a scalar particle is not protected by symmetry. The mass of the Standard Model (SM) fermion, for example, is protected by the chiral symmetry [1] [2].

2 Hierarchy problem

This section is based on lectures given by F. Brümmer in the DESY summerstudent programme [1].

The Hierarchy problem arises when we consider extensions of the standard model. Since the SM does not include gravity, it is expected that it can not be correct up to scales larger than the Planck scale (10^{18} GeV). The Planck scale is the scale where gravity becomes as strong as the SM forces (electro-weak and strong force).

The SM is thus expected to be an effective field theory (EFT) which breaks down at the latest at the Planck scale. In order to describe physics above that scale we need a UV completion of the theory. An example of an EFT is, for instance, the Fermi theory, which is an effective theory for the electro-weak interactions at energies much below the W and Z mass.

To see how the Hierarchy problem arises in BSM theories we will discuss one of the simplest extensions of the SM (called type 1 seesaw). This model adds a right handed neutrino (ν_R) of mass M to the SM. This results in the following Lagrangian (assuming only one family):

$$\mathcal{L} = \mathcal{L}_{SM} + \nu_R i \not{\partial} \nu_R + \frac{1}{2} M \nu_R \nu_R + \text{h.c.} + y H l_L \nu_R + \text{h.c.} \quad (1)$$

The first term is just the SM Lagrangian. The second term is the kinetic term for the right-handed neutrino. The third term is a Majorana mass term for the right-handed neutrino. The last term is the Yukawa interaction between the left-handed leptons (neutrino and electron), the right-handed neutrino and the Higgs doublet H . y is the Yukawa coupling strength. When the Higgs field gets a non-zero vev (v), a Dirac mass term is created which gives the neutrinos a mass of yv .

The new physics scale is given by M , with $M \gg v$. For low energy processes ν_R will only contribute to processes as a virtual particle since the energy available is not enough to create a real ν_R .

The term $y H l_L \nu_R$ has an important effect when we consider the 1-loop self interaction of the Higgs. It results in an interaction of the form:

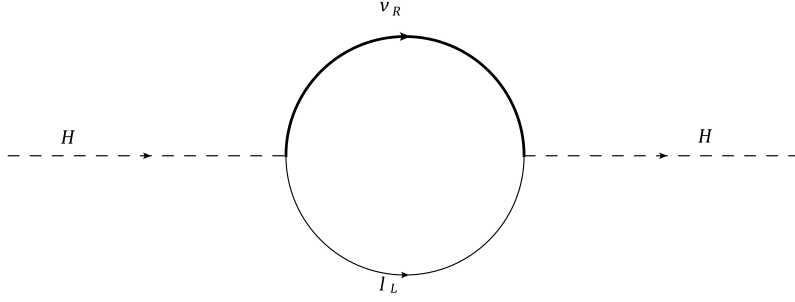


Figure 1: Radiative corrections to the Higgs mass from right handed neutrino

If we add this term and construct the physical mass of the Higgs we get:

$$m_{\phi, \text{eff}}^2 = m_{\phi}^2 - \frac{y^2}{8\pi^2} M^2 \quad (2)$$

Assuming a Yukawa coupling of $\mathcal{O}(1)$, M is fixed by the tiny mass of the neutrino to 10^{13} GeV. The physical Higgs mass is $\mathcal{O}(100 \text{ GeV})$, namely 125 GeV.

Thus, in order to obtain a Higgs mass similar to what we see in observations, the two terms on the right of equation 2 must cancel with a precision of 1 part in $\sim 10^{24}$. This extreme fine-tuning of parameters is called the (electroweak) Hierarchy problem. This is a general problem for UV completions of the SM and not specific to the model explained above.

To summarize; the Hierarchy problem arises when viewing the SM as an effective field theory. When we take into account new states with $M \gg v$, loop corrections of these states to the Higgs mass result in large counter terms to the Higgs mass. To still get a small value for the physical Higgs mass, like we see in experiments (125 GeV), extreme fine-tuning is needed.

3 Relaxation model

The Relaxion model is based on the interaction between an axion field and the Higgs field, the potential describing this is the following [3]:

$$V(\phi, h) = \lambda h^4 + (-M^2 + g\phi)h^2 + gM^2\phi + \Lambda^4 \cos(\phi/f) \quad (3)$$

where g is a coupling and it is responsible for the breaking of the shift symmetry $\phi \rightarrow \phi + 2\pi f$, M is the cut-off of the theory and $\Lambda^4 = \mu^3 h$.² μ is related to an energy scale and is needed to get the dimensions correct. For the Quantum Chromodynamics (QCD) axion μ is related to the QCD scale, Λ_{QCD} . f is the decay constant of the axion. h is the vev of the doublet defined as:

$$H = \frac{1}{\sqrt{2}} \begin{pmatrix} 0 \\ h \end{pmatrix} \quad (4)$$

This potential is also shown in fig. 2.

We see that for $\phi < M^2/g$ the Higgs mass is negative. This will result in spontaneous symmetry breaking and will give the Higgs mass a non-zero vev. The vev is given by (neglecting the contribution of the oscillatory term):

$$h(\phi) = \begin{cases} \sqrt{\frac{M^2 - g\phi}{2\lambda}}, & \phi < \frac{M^2}{g} := \phi_c \\ 0 & \text{otherwise.} \end{cases} \quad (5)$$

Using the FLRW metric, the evolution of ϕ will be governed by Friedmann equation:

$$\ddot{\phi} + 3H_I \dot{\phi} + V'_\phi = 0, \quad (6)$$

where H_I is the Hubble constant during inflation.

Now, before choosing the values of the constants, we will derive some constraints [3] that are essential for the model to have a physical meaning.

The Hubble friction must be such that it allows the axion field to slow-roll. Moreover, the vacuum energy during inflation ρ_{inf} should be greater than the vacuum energy change along the $V(\phi)$ potential, ρ_ϕ . Then:

$$\frac{(\dot{\phi})^2}{2} \ll \rho_\phi \implies \begin{cases} \frac{(V'(\phi)/(3H_I))^2}{2} \ll V(\phi) \simeq gM^2 \left(\frac{M^2}{g} \right) \implies g \ll H_I \\ \frac{(V'(\phi)/(3H_I))^2}{2} \ll \rho_\phi \lesssim \rho_{\text{inf}} = 3H^2 M_{pl}^2 \implies g \ll H_I^2 \frac{M_{pl}}{M^2} \end{cases} \quad (7)$$

$$H_I^2 = \frac{\rho_{\text{inf}}}{3M_{pl}^2} \gtrsim \frac{M^4}{3M_{pl}^2} \implies H_I \gtrsim \frac{M^2}{M_{pl}} \quad (8)$$

²Note that in the full Lagrangian we should not only have the term $\sim gM^2\phi$ but all terms of the expansion $M^4(g\phi/M^2 + (g\phi/M^2)^2 + \dots)$. To simplify the simulations done these terms will be ignored.

We need slow-roll to ensure both that the dynamics is independent of the initial condition of the field ϕ and that ϕ does not overshoot the bumps created by Higgs vev. When slow-roll is satisfied, the kinetic energy which is gained by going down the potential is taken away by the Hubble friction, thus making the initial value of ϕ irrelevant.

Moreover, we have to assure that the evolution is dominated by classical rolling. In one e-fold, quantum fluctuations of the size H_I should be less important than the classical change of the field given by: $\Delta\phi \sim \dot{\phi}/H_I \sim V'_\phi/(3H_I^2)$. Hence,

$$H_I \lesssim (gM^2)^{1/3} \quad (9)$$

The slow-rolling of the axion will stop when the slope of the barriers Λ^4/f becomes of the order of the slope of the potential gM^2 :

$$v \sim \frac{gM^2 f}{\mu^3} \implies \phi_{end} \sim \phi_c - \frac{2\lambda g M^4 f^2}{\mu^6} \quad (10)$$

Thus, when taking the values of the constant so as to simulate the dynamics of the axion-field under this potential, we will choose μ to be such that ϕ gets stuck at $\phi \sim 0.9\phi_c$, which corresponds to a Higgs vev of $v^2 = \frac{0.1M^2}{2\lambda}$. So as to get the expected Higgs vev, we will use $\lambda = \frac{0.1M^2}{v^2}$, with $v = 246$ GeV.

The potential is plotted in figure 2 and a zoom-in is plotted in 3.

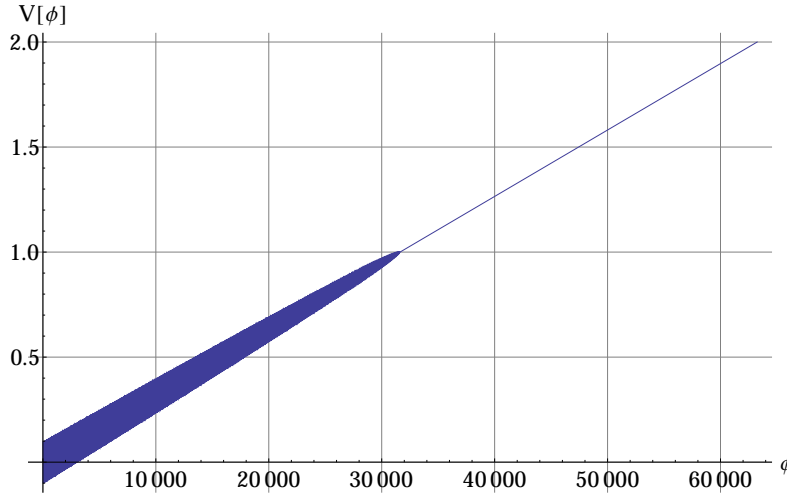


Figure 2: Potential with values $M = 1$, $f = 10$, $H = 10^{-3}$ and $g = 10^{-4.5}$ (in units of 10 TeV). To be able to distinguish the bumps of the potential, we have multiplied the oscillatory term by 100.

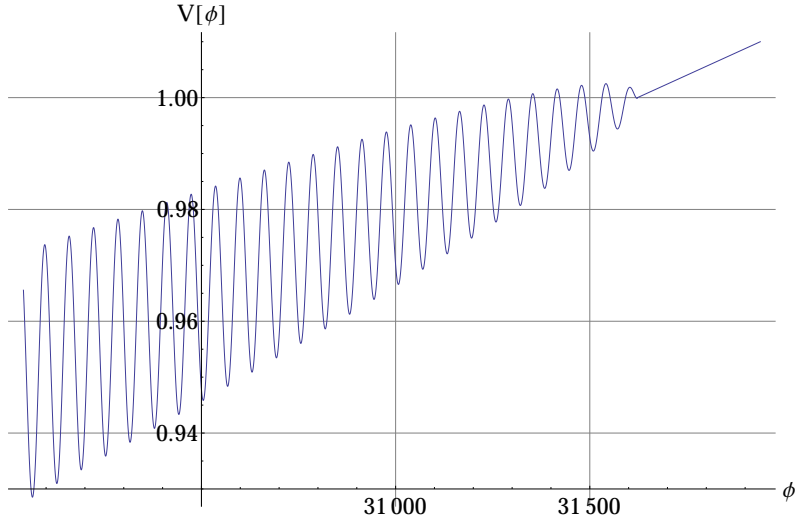


Figure 3: Zoom-in of the previous plot between $0.95 M^2/g$ and $1.01 M^2/g$

Using Mathematica we simulate the dynamics by solving equation 6 with the potential given by equation 3. The dynamics of the field ϕ as a function of t is shown in figure 4. We clearly see the field getting over several bumps before it gets stuck in a certain minimum of the potential.

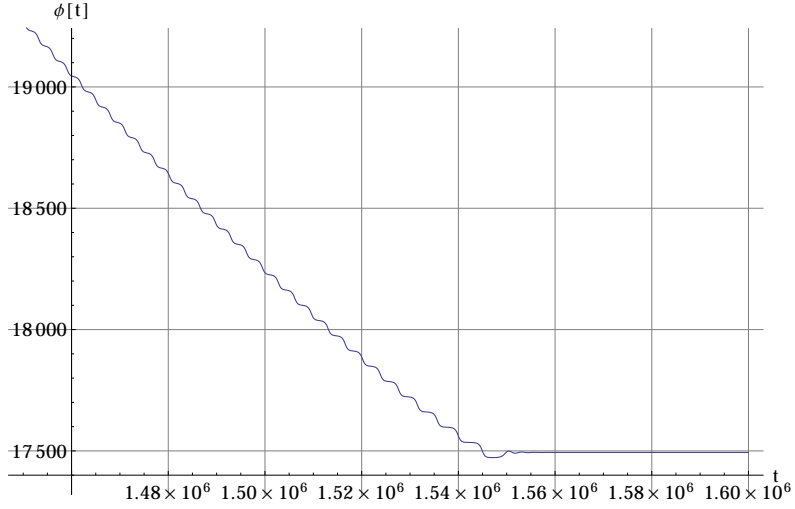


Figure 4: Temporal evolution of field ϕ .

By solving the equation in one step, we encountered some numerical problems and singularities. Since a likely cause for this is the fact that we are trying to solve over a too large range for ϕ , we tried to solve it iteratively. This resulted in the ability to solve the

dynamics for g from this initial value to $g = 10^{-6}$. Using these methods, we were able to reach a minimum after passing almost 2000 bumps. Having passed lots of bumps means that the minima are closely spaced together. Thus, in order to have a small value for the Higgs vev, it is not important to end up in a specific minimum. A range of minima will result in more or less similar value for the Higgs vev.

The final position of the field ϕ is plotted for different values of g in figure 5.

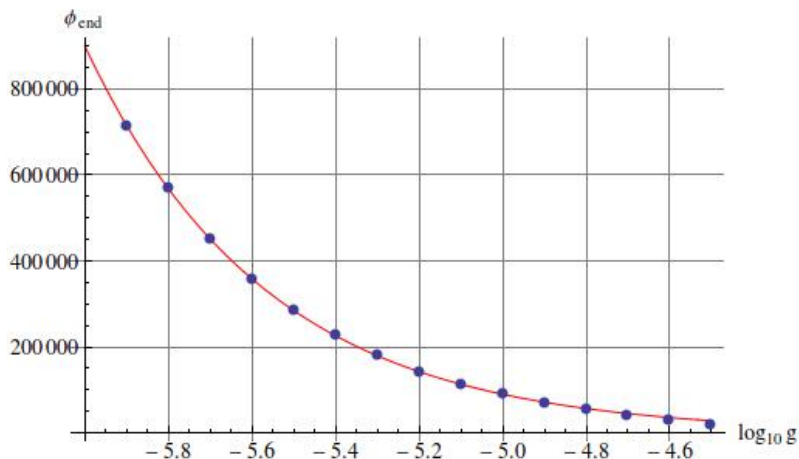


Figure 5: Final position of the field ϕ (minimum where it gets eventually stuck) in function of $\log_{10}(g)$. It coincides almost perfectly with the red line corresponding to the function $0.9M^2/g$, which was imposed when choosing the parameter μ .

4 Double scanner mechanism

The problem with the original model is that the axion field used is the QCD axion, originally used to solve the strong CP problem [5]. The original Relaxion model however predicts a charge-parity (CP) parameter of $\theta \sim 1$, which is in contradiction with the observed value, $\theta \sim 10^{-10}$ [3].

To solve this, but keep a term $\sim |h|$, a new strong group can be proposed [3]. However, this will result in an extra source of electro-weak symmetry breaking. To avoid these problems in [4] another solution is proposed. Instead of $\sim |h|$, as coefficient in front of the cosine term, we take a term $\sim |h|^2$. This however creates quantum corrections at the loop level which need to be dealt with. To show how these quantum corrections arise, we will start with a potential similar to the original model:

$$V(\phi, H) = \Lambda^3 g \phi - \Lambda^2 \left(\alpha - \frac{g\phi}{\Lambda} \right) |H|^2 + \epsilon \Lambda^2 |H|^2 \cos(\phi/f) \quad (11)$$

where Λ is the UV cut-off scale of the model, $0 < g \ll 1$ is a dimensionless constant and is as before the responsible for the symmetry breaking $\phi \rightarrow \phi + 2\pi f$, α is an $\mathcal{O}(1)$ positive coefficient and $\epsilon \ll 1$ is a dimensionless constant that controls the amplitude of the oscillating term.

Quantum corrections will generate terms of the form $\sim \epsilon \Lambda^4 \cos(\phi/f)$ and $\sim \epsilon \Lambda^3 g \phi \cos(\phi/f)$ [4]. To see this we will first look at the two interaction vertices of this potential:

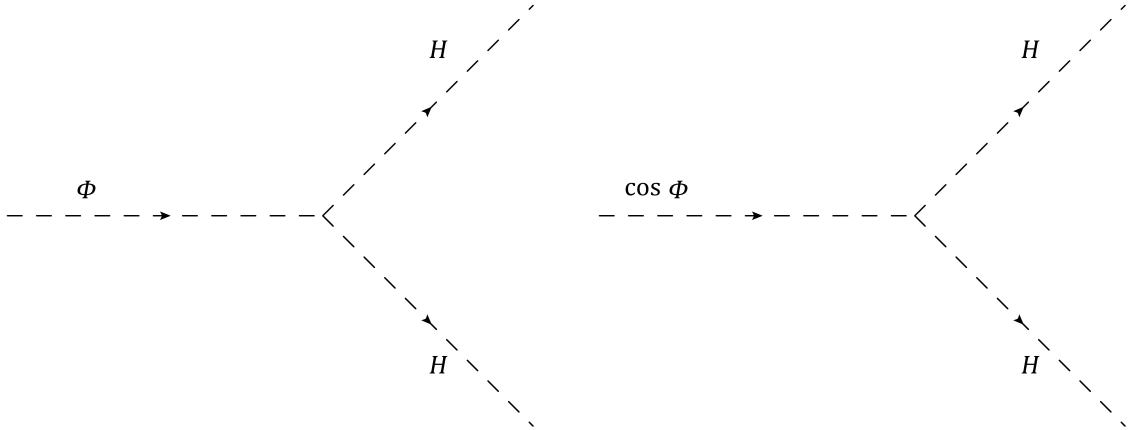


Figure 6: Vertices $g\Lambda\phi|H|^2$ (left) and $\epsilon\Lambda^2|H|^2\cos(\phi/f)$ (right)

Radiative corrections are the result of closing loops. This results in the following diagrams:

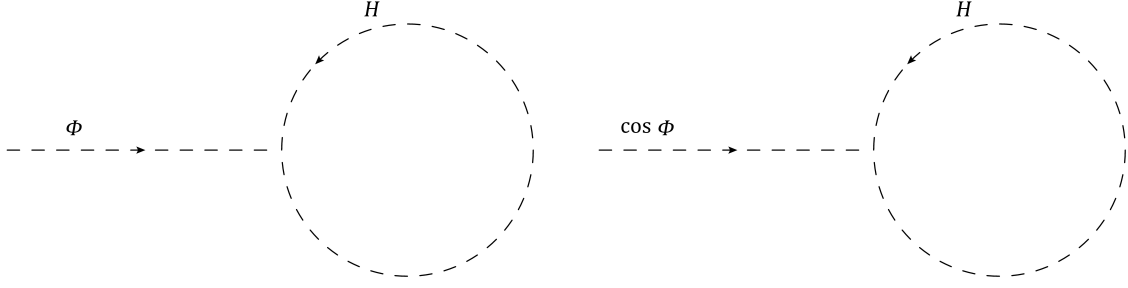


Figure 7: Closing loops of the diagrams in figure 6

These loop diagrams contribute the following terms to the potential; a loop means we have to integrate the propagators over the independent momenta. Since the loops contain one scalar propagator and one independent momentum, we end up with an integral of the form $\int_0^\Lambda d^4p \frac{1}{p^2}$, where we have neglected masses and constants. Using only dimensional analysis and neglecting constants, this integral will be of order $\sim \Lambda^2$. Taking into account the interaction strength, we end up with:

$$g\Lambda\phi \int_0^\Lambda d^4p \frac{1}{p^2} \sim g\Lambda^3\phi$$

for the left diagram, which adds nothing to the potential since this term was already present. And:

$$\epsilon\Lambda^2 \cos(\phi/f) \int_0^\Lambda d^4p \frac{1}{p^2} \sim \epsilon\Lambda^4 \cos(\phi/f)$$

for the right diagram. This will create bumps which are already present before the Higgs vev creates bumps. This term will thus cause the field to get stuck before the critical value is reached. Other quantum corrections terms can be created by combining the two vertices as follows:

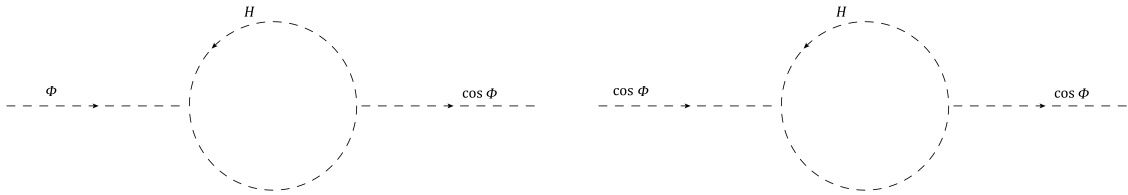


Figure 8: Other quantum corrections

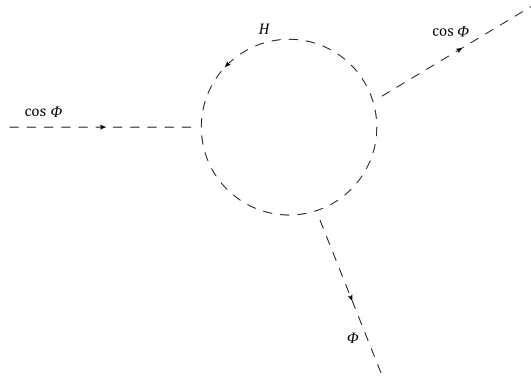


Figure 9: Some other quantum corrections

In a similar way as explained before, this will create the following terms in the potential [4].

For the left diagram of figure 8 we get:

$$g\phi\Lambda\epsilon\Lambda^2\cos(\phi/f)\int_0^\Lambda d^4p\frac{1}{p^4}\sim\epsilon g\Lambda^3\phi\cos(\phi/f)$$

For the right diagram of figure 8 we get:

$$(\epsilon\Lambda^2\cos(\phi/f))^2\int_0^\Lambda d^4p\frac{1}{p^4}\sim\epsilon^2\Lambda^4\cos^2(\phi/f)$$

For the diagram of figure 9 we get:

$$g\phi\Lambda(\epsilon\Lambda^2\cos(\phi/f))^2\int_0^\Lambda d^4p\frac{1}{p^6}\sim\epsilon^2g\Lambda^3\phi\cos^2(\phi/f)$$

So we end up with four quantum corrections terms, two of these are of order ϵ and the other two of order ϵ^2 . These terms will destroy the dynamics of the model. In order to solve this, [4] introduces a second axion field which then screens both terms generated by $\mathcal{O}(\epsilon)$ quantum corrections. The $\mathcal{O}(\epsilon^2)$ corrections will be dealt with by imposing a specific constraint, as discussed later on.

Adding this extra field results in the following potential [4]:

$$V(\phi, \sigma, H) = \Lambda^4\left(\frac{g\phi}{\Lambda} + \frac{g_\sigma\sigma}{\Lambda}\right) - \Lambda^2\left(\alpha - \frac{g\phi}{\Lambda}\right)|H|^2 + A(\phi, \sigma, H)\cos(\phi/f) \quad (12)$$

$$A(\phi, \sigma, H) = \epsilon\Lambda^4\left(\beta + c_\phi\frac{g\phi}{\Lambda} - c_\sigma\frac{g_\sigma\sigma}{\Lambda} + \frac{|H|^2}{\Lambda^2}\right)$$

where $g_\sigma \ll 1$ is a dimensionless coupling to the σ -axionfield and β , c_ϕ , c_σ are $\mathcal{O}(1)$ dimensionless positive coefficients.

Important here are the terms in A . The three extra terms are the quantum corrections from σ and ϕ . We imagine the evolution to go as follows [4]:

We start with initial values for ϕ and σ , such that the Higgs vev is zero and A is large, this will result in large bumps; ϕ will be stuck in a minimum. σ will slow-roll down its own potential since it does not feel the bumps ³.

This will decrease the steepness of the bumps, thus making it possible for ϕ to get out of the minimum and start slow roll. This will go on until, like in the previous example, the Higgs vev obtains a non zero expectation value and ϕ gets stuck in another minimum, below the critical value. In the end the result is a value for the Higgs vev which can be much smaller than the scale of new physics, without the need of any fine-tuning.

The Higgs vev is given in the following formula, where we again ignore the oscillatory term:

$$H^2(\phi) = \begin{cases} \frac{\Lambda^2(\alpha - \frac{g\phi}{\Lambda})}{2\lambda}, & \phi > \frac{\Lambda}{g}\alpha := \phi_c \\ 0 & \text{otherwise.} \end{cases} \quad (13)$$

In order for the field ϕ to have the behavior as explained and end up in minimum close to the critical value some conditions must be fulfilled. Firstly we have the condition that the steepness of the oscillatory term is smaller than the one from $\Lambda^3 g \phi$. This is to make sure that the Higgs field scans a large enough range and does not get stuck at the first bump. This results in the following inequality:

$$\left| \frac{1}{f} A(\phi_*, \sigma, H(\phi_*)) \right| \lesssim g \Lambda^3$$

which trivially leads to these values:

$$\phi_* \in \begin{cases} \phi_c + \frac{c_\sigma g_\sigma}{c_\phi g} (\sigma - \sigma_c) \pm \frac{f}{c_\phi \epsilon}, & \phi_* > \phi_c \\ \phi_c + \frac{c_\sigma g_\sigma}{c'_\phi g} (\sigma - \sigma_c) \pm \frac{f}{c'_\phi \epsilon} & \text{otherwise.} \end{cases} \quad (14)$$

$$c'_\phi = c_\phi - 1/(2\lambda) \quad \sigma_c = (g c_\phi \phi_c + \beta \Lambda)/(c_\sigma g_\sigma)$$

³Because the oscillating potential is only dependent on ϕ not on σ . In the Friedman equation for σ there will thus be no contribution from the oscillatory term

To make sure that ϕ remains in this zone when it rolls down and does not get stuck in another minimum before reaching the critical value ϕ_c , it has to fulfill the following condition:

$$\frac{g}{g_\sigma} = \frac{d\phi(t)/dt}{d\sigma(t)/dt} > \frac{d\phi_*}{d\sigma} = \frac{c_\sigma g_\sigma}{c_\phi g} \implies c_\phi g^2 > c_\sigma g_\sigma^2 \quad (15)$$

Once $\phi \leq \phi_c$, ϕ must exit the band so as to get trapped in some vacuum. Then, if $c'_\phi > 0$

$$\frac{g}{g_\sigma} < \frac{c_\sigma g_\sigma}{c'_\phi g} \implies c'_\phi g^2 < c_\sigma g_\sigma^2 \quad (16)$$

As for the case when $c'_\phi < 0$, since both slopes have different signs, the field ϕ will trivially exit the band and finally get trapped in a minimum.

Moreover, we have to ensure that quantum correction terms like $\epsilon^2 \Lambda^4 \cos^2(\phi/f)$ are negligible:

$$\epsilon \lesssim v^2/\Lambda^2, \quad (17)$$

where v is the Higgs vev where it gets stuck, which analogously as in the former model is the point where the slope of the oscillatory term and linear term coincide:

$$v^2 \simeq \frac{g\Lambda f}{\epsilon} \quad (18)$$

The energy density carried by the axion fields is smaller than the inflation scale ρ_{inf} :

$$H_I = \frac{\sqrt{\rho_{\text{inf}}}}{\sqrt{3}M_{pl}} \gtrsim \frac{\Lambda^2}{\sqrt{3}M_{pl}} \implies H_I \gtrsim \frac{\Lambda^2}{M_{pl}} \quad (19)$$

The condition for classical rolling is that quantum fluctuations of size H_I remain smaller than classical field displacements over one Hubble time:

$$\Delta\sigma \sim H_I^{-1}\dot{\sigma} \sim H_I^{-2}V_\sigma/3 \gtrsim H_I \implies H_I^3 \lesssim g_\sigma \Lambda^3 \quad (20)$$

From Eq. 17-20, we trivially get these bounds for g :

$$\frac{\Lambda^3}{M_{pl}^3} \lesssim g_\sigma \lesssim g \lesssim \frac{v^4}{f\Lambda^3} \quad (21)$$

In order to simulate all the stages of the slow-rolling of both axion fields, we have to start with a potential with two points (below and above ϕ_c) where the amplitude of the oscillating term is zero. These two points are given by the following expressions:

$$\begin{cases} \min_I(\sigma) = \frac{c_\sigma g_\sigma \sigma - \beta \Lambda}{g c_\phi}, \\ \min_{II}(\sigma) = \frac{c_\sigma g_\sigma \sigma - \beta \Lambda - \frac{\alpha \Lambda}{2\lambda}}{g c'_\phi} \end{cases} \quad (22)$$

So that $\min_{II}(\sigma_0) < \phi_c < \min_I(\sigma_0)$ we have to fulfill the following conditions:

$$c'_\phi < 0, \quad \frac{c_\sigma \sigma_0 g_\sigma}{\Lambda} - \beta > \alpha c \quad (23)$$

We have verified that the following constants fulfill all our constraints:

For the dimensionless coefficients:

$$\alpha = c_\phi = c_\sigma = 1, \quad \lambda = 10^{-1}$$

And for the dimensionful parameters, in units of GeV:

$$\Lambda = f = 10^3, \quad g = 10g_\sigma = 10^{-3}, \quad 3H_I = 40.$$

So as to get the Higgs value $v = 246$ GeV, we will simply use $\epsilon = \frac{\Lambda^2 g}{v^2}$, which fulfills as well Eq. 17.

Figure 10 shows the potential for $\sigma = 1.5 \frac{\Lambda}{g_\sigma}$. The two points where the amplitude of the oscillating term vanishes have been marked with a black dot.

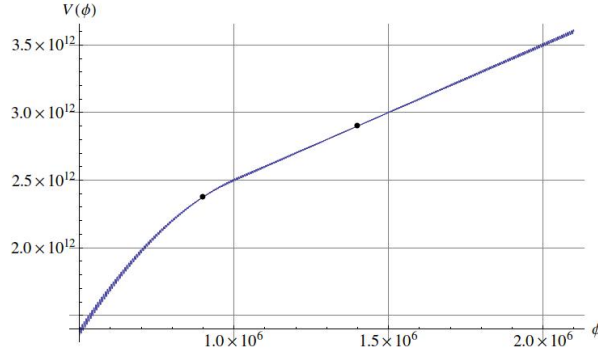


Figure 10: Potential for $\sigma_0 = 1.5 \frac{\Lambda}{g_\sigma}$.

Now, we are able to solve the Friedmann equation for ϕ and σ . Starting at an initial value of ϕ just between the two black dots ($\phi_0 = 1.2\phi_c$) and an initial value of σ given by $1.5 \frac{\Lambda}{g_\sigma}$.

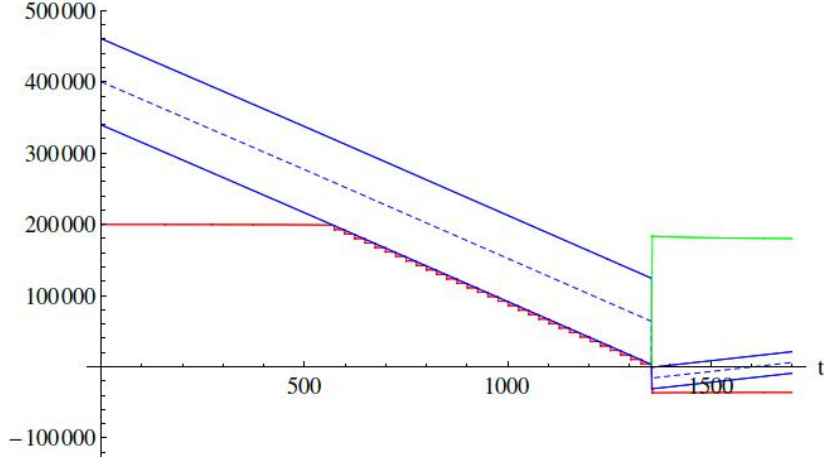


Figure 11: Evolution of axion field ϕ .

In Fig 11, we have represented in red $\phi - \phi_c$, clearly seeing the different stages in which it is involved. Firstly, it stays on the initial value until the slow-roll of the field σ enables this point to coincide with the vanishment of the amplitude. Then, the field ϕ is able to slow-roll until reaching the critical value within the allowed region of Eq. 14 (in blue).

Just after it crosses the critical value, it gets stuck in one minimum getting here out of the allowed region of Eq. 14 and such that the Higgs vev (v^2 , in green) gets activated. The final Higgs vev is $v \simeq 424$ GeV, which is of the same order of magnitude as the expected value $v = 246$ GeV.

In the next figures, we can see how the field ϕ slow-rolls down the potential:

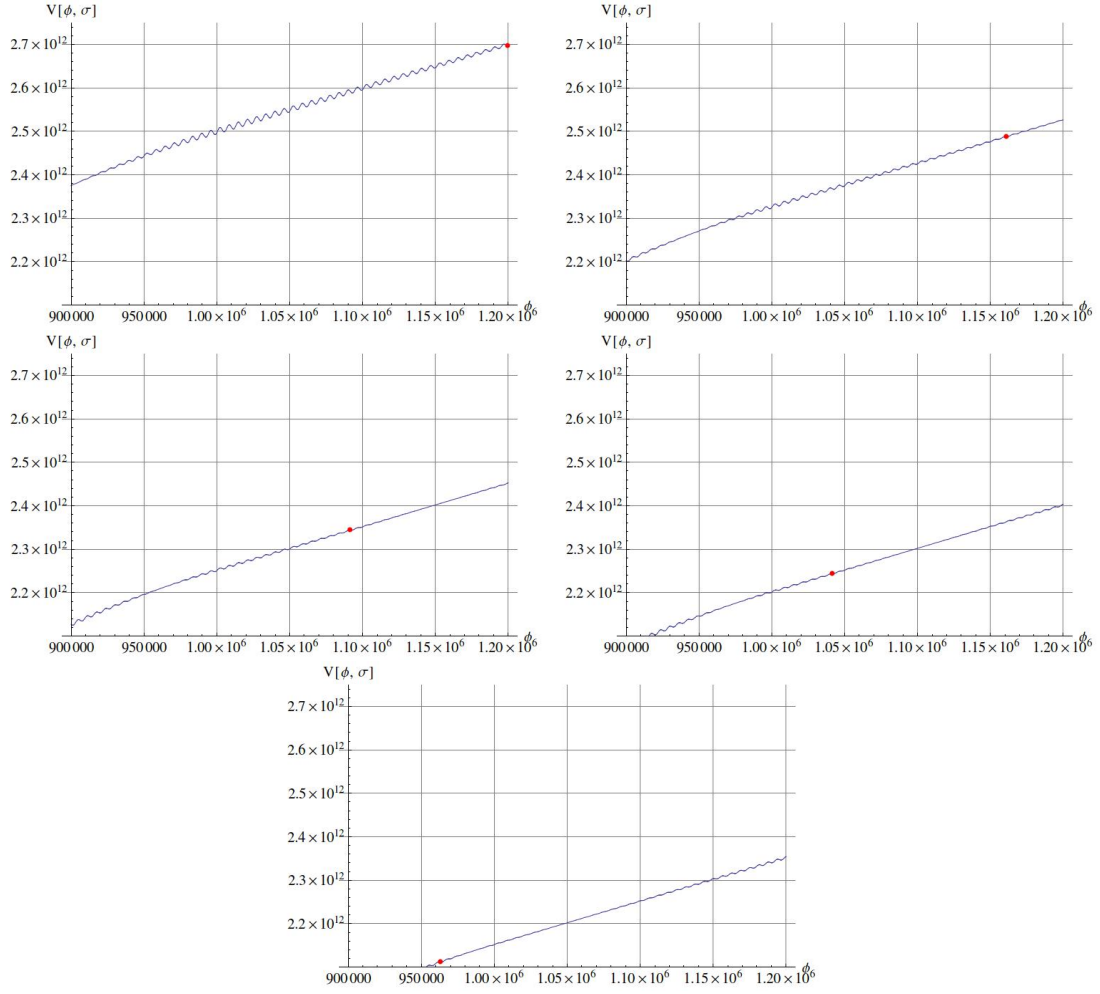


Figure 12: Evolution of field ϕ , for $t = 0$ (top left), $t = 700$ (top right), $t = 1000$ (middle left), $t = 1200$ (middle right) and $t = 1400$ (bottom)

We see that it coincides well with the expected behaviour. We also see that the Higgs field ends up in a minimum smaller than, but close to the critical value ($1.0 \cdot 10^6$).

5 Superradiance

Axion or axion-like particles pop up in several BSM theories to solve current problems in the SM. The problems range from the strong CP problem to the cosmological constant problem. As explained above, the existence of light axions is also a proposed solution to the electroweak hierarchy problem. Most BSM theories predict one or several axions. The following figure shows a plot of the cross section and mass of some of the proposed axions.

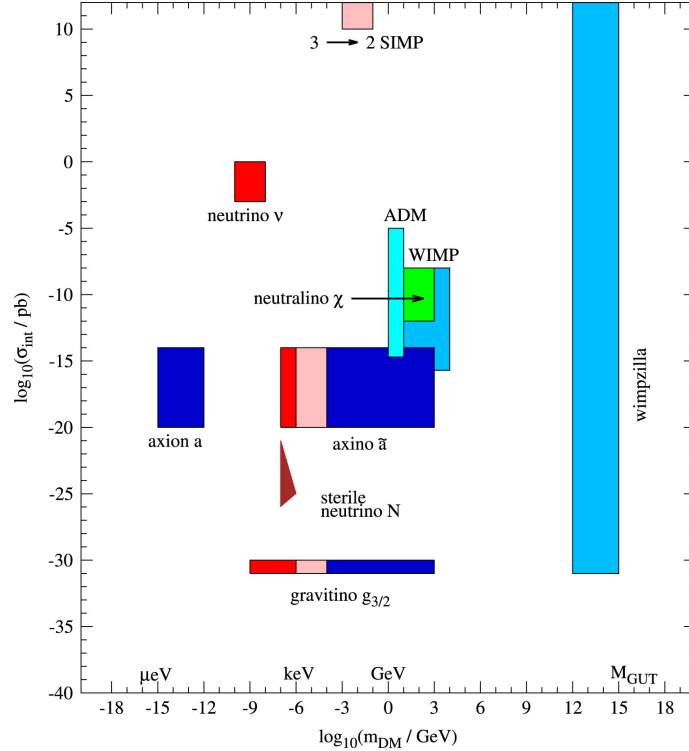


Figure 13: Proposed axions [6]

In order to test these theories, we need (in)direct evidence for their existence and we need to measure their mass. One possible way to detect axions are the “light shining through a wall” experiments, like the ALPS experiment at DESY [7]. Another method would be through the effect of superradiance [8] [9]. Superradiance is the effect by which, when an axion scatters from a rotating (Kerr) BH, the reflected wave has a larger amplitude than the incoming wave. Rotating black holes are not the only type of system where this occurs, but however they are the one in which the superradiance of bosonic particles can be better observed [8].

Light axions can bind to a Kerr black hole and form a cloud around it, called a gravitational atom. This only happens when the BH size is of the same order as the Compton wavelength of the axion [8]. When this happens, the axions extract energy/spin from the BH, thus causing the BH to lose energy (spin-down). We will show that these axions will have a specific effect on the distribution of BH's and thus the effect of superradiance can be used to detect axions. The properties of BH's, like spin and mass, can be determined from Gravitational Wave detections.

5.1 Kerr Black Holes

According to the no-hair theorem, all black hole solutions of the Einstein equations are completely defined by three classical parameters: mass, electric charge and angular momentum [10].

Here, we are going to deal with Kerr metric, which enables us to describe black holes with angular momentum J . Using Boyer-Lindquist coordinates, the metric expression is the following [11]:

$$ds^2 = - \left(1 - \frac{2GMr}{\rho^2}\right) dt^2 - \frac{4GMr a \sin^2 \theta}{\rho^2} d\varphi dt + \frac{\rho^2}{\Delta} dr^2 + \rho^2 d\theta^2 + \left(r^2 + a^2 + \frac{2GMr a^2 \sin^2 \theta}{\rho^2}\right) \sin^2 \theta d\varphi^2 \quad (24)$$

$$a \equiv \frac{J}{GM}, \quad \rho^2 \equiv r^2 + a^2 \cos^2 \theta, \quad \Delta \equiv r^2 - 2GMr + a^2, \quad a^* \equiv \frac{a}{r_g} \equiv \frac{a}{GM}$$

being G the gravitational constant and M the BH mass. We obtain the singularities of the black hole by setting Δ to 0:

$$r^\pm = r_g \left(1 \pm \sqrt{1 - a^{*2}}\right) \quad (25)$$

Since the outer horizon r^+ only exists for $a^* \leq 1$, we have a maximum angular momentum for $a_{max}^* = 1$. For stationary observers ($u_{\text{obs}}^\mu = (u_{\text{obs}}^0, 0, 0, 0)$), we have that $u_{\text{obs}}^2 = -g_{00}(u_{\text{obs}}^0)^2 = -1$, which can only be satisfied for $r \leq r_e^+(\theta)$, the outer ergosphere (region where $g_{00} = 0$):

$$r_e^\pm(\theta) = r_g \left(1 \pm \sqrt{1 - a^{*2} \cos^2 \theta}\right) \quad (26)$$

Once a particle enters the outer ergosphere, it is forced to move in the tangential direction and dragged by the rotating black hole, but however it is not forced towards the black hole center. This happens only when the outer horizon is reached; from there on particles are always moving towards the black hole center. Figure 14 shows the different regions around a Kerr black hole.

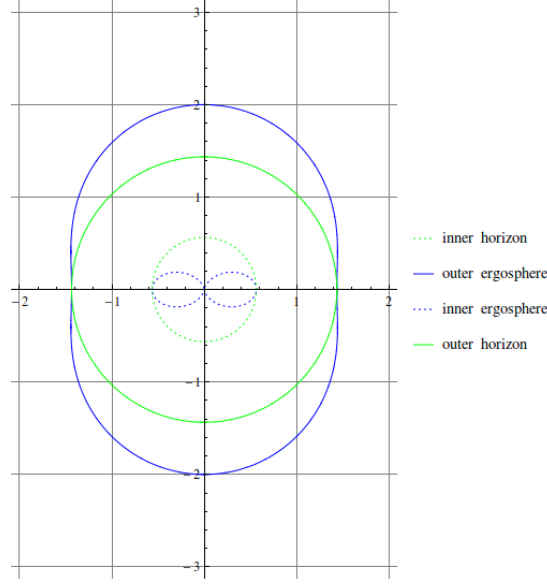


Figure 14: Regions of a Kerr black hole with $a^* = 0.9$ and $r_g = 1$.

5.2 Superradiance condition

We can establish a clear analogy between the system formed by a black hole of mass M and radius r_g and a massive boson of mass μ_a and the hydrogen atom [8]. It can be called a gravitational atom [8] with quantum energy levels specified by $\{n, l, m\}$ and energies given by:

$$\omega \simeq \mu_a \left(1 - \frac{\alpha^2}{2n^2} \right) \quad (27)$$

The zone where superradiance is possible corresponds to the region inside the plane M_{bh} versus μ_a where Compton wavelength of the axion $\lambda_a = \frac{h}{c\mu_a}$ (which in natural units is $\lambda_a = \frac{2\pi}{\mu_a}$) is comparable to r_g :

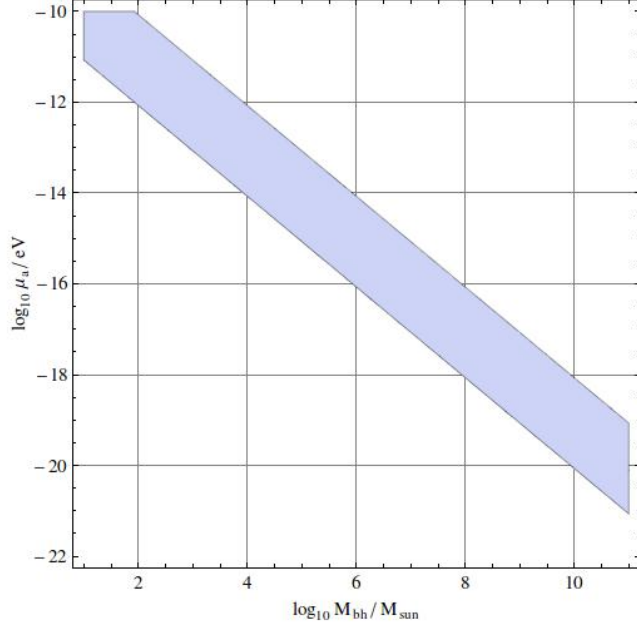


Figure 15: Superradiance zone in the plane $\log_{10}(\mu_a/eV)$ versus $\log_{10}(M_{\text{BH}}/M_{\odot})$. We will consider that λ_a is comparable to r_g if $r_g/10 < \lambda_a < 10r_g$.

We see that for BH ranging from several M_{\odot} to $100M_{\odot}$, superradiance is possible for axion masses between 10^{-22} to 10^{-10} . Looking back at figure 13 we see that a large range of this axion plot can be investigated using superradiance.

The superradiance condition for a level with energy ω and magnetic quantum number m is:

$$\frac{\omega}{m} < \omega^+, \quad \omega^+ \equiv \frac{1}{2} \left(\frac{a^*}{1 + \sqrt{1 - a^{*2}}} r_g^{-1} \right) \quad (28)$$

The superradiance rate has also to be fast enough to grow a maximally filled cloud:

$$\Gamma_{\text{sr}} \tau_{\text{BH}} \geq \log N_{\text{max}} \quad , \quad (29)$$

where $N_{\text{max}} \simeq \frac{G_N M_{\text{BH}}^2}{m} (1 - a^*)$ is the maximum number of bosons occupying the level, τ_{bh} is the shortest time in which superradiance can be disturbed, which we will take as $\tau_{\text{Eddington}}/10 = 4 \cdot 10^7$ years, and the superradiance rate, using the non-relativistic approximation from [12] ($\alpha/l \ll 1$), has the following expression:

$$\Gamma_{\text{sr}}^{lmn} = 2\mu\alpha^{4l+4} r^+ (m\omega^+ - \mu_a) C_{lmn} \quad (30)$$

$$C_{lmn} = \frac{2^{4l+2} (l+n)!}{n^{2l+4} (n - (l+1))!} \left(\frac{l!}{(2l)! (2l+1)!} \right)^2 \prod_{j=1}^l (j^2 (1 - a^{*2}) + 4r^{+2} (m\omega^+ - \mu_a)^2)$$

We will always consider $m = l = n - 1$. The figure below shows Γ_{sr} as a function of μ_a for different values of l .

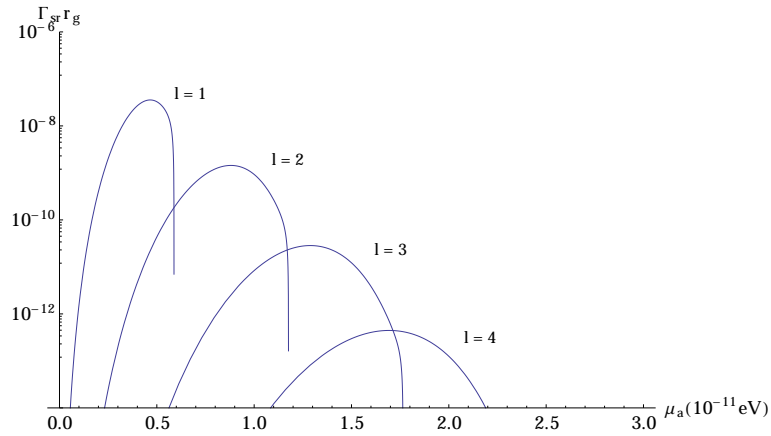


Figure 16: $\Gamma_{sr} r_g$ in function of μ_a (in eV), with $a^* = 0.99$ and $M_{\text{BH}} = 10M_{\odot}$ for $l=1$ to $l=4$ from left to right.

Figure 17 shows the regions in the (M_{BH}, a^*) plane where superradiance occurs, for the different l levels.

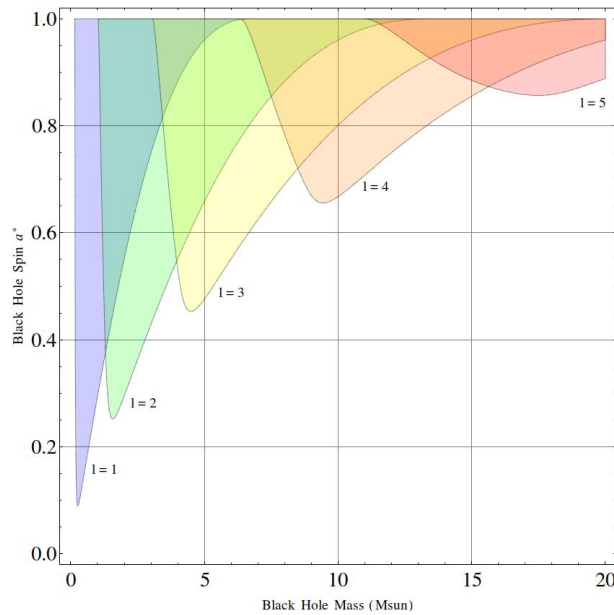


Figure 17: Superradiance regions in the plane M_{BH}/M_{\odot} versus spin a^* for $l=1$ to $l=5$ from left to right.

We expect the following dynamics. Let us have a black hole with mass M_{BH} and spin a_0^* and we initially have a cloud of $N_{\text{max}}(a_0^*)$ axions. The initial quantum number l will be the smallest possible such that the point (M_{BH}, a_0^*) fulfills the superradiance conditions.

Then, the number of axions will evolve in the following way [8]:

$$\frac{dN}{dt} = \Gamma_{sr} N \quad (31)$$

extracting spin from the black hole by $a^* = N_{\text{max}}^{-1}(N)$.

When reaching the point (M_{BH}, a^*) where the superradiance condition is not valid anymore for this l , axions will annihilate into gravitons until reaching $N_{\text{max}}(a^*)$ for the next quantum level.

$$\frac{dN}{dt} = -\Gamma_a N^2 \quad (32)$$

$$\Gamma_a \simeq 10^{-10} (2\alpha/l)^p \frac{G_N}{r_g^3}, \quad \text{where } p = \begin{cases} 17, & l = 1 \\ 4l + 1, & l \geq 2. \end{cases}$$

Afterwards, the number of axions will again increase by superradiance and the process will repeat until reaching the zone where the superradiance condition does not hold for any l .

We have computed these dynamics for a cloud of axions of $\mu = 10^{-11}$ eV around a black hole of $M_{\text{BH}} = 6M_\odot$ and initial spin $a_0^* = 0.95$, thus starting in $l = 2$ region. There are three stages:

- The number of axions increase exponentially until having extracted enough spin to the black hole so as to exit the superradiance zone for $l = 2$ (~ 0.13 years).
- Then, axions are annihilated into gravitons until reaching some critical value ($\sim 1.9 \cdot 10^5$ years).
- Finally, level $l = 3$ becomes populated until leaving its superradiance zone (~ 1600 years).

5.3 Distribution of black holes

To show the effect of superradiance on the BH distribution we first consider the probability of finding a black hole of a certain mass. In [13] a Bayesian analysis of observed masses of binary systems is done which resulted in the following BH distribution:

$$P(M) = M_0^{-1} e^{(M_{\text{min}} - M)/M_0} \quad (33)$$

where $M_{min} = 5.3M_{\odot}$ and $M_0 = 4.7M_{\odot}$.

Then, considering that the spin distribution is flat [8], the expected distribution for 10^4 black holes would be:

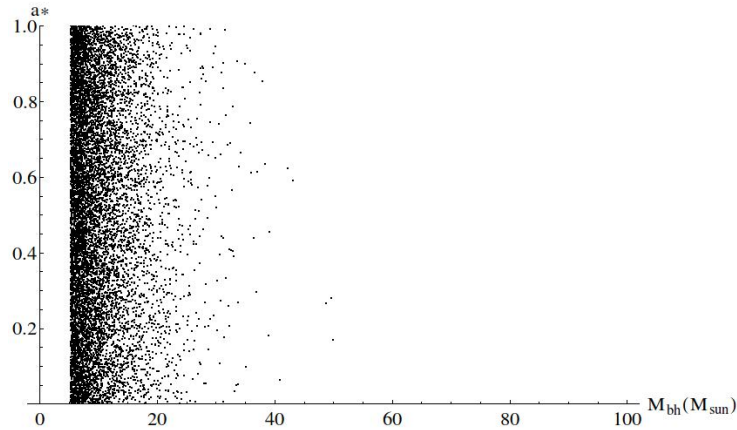


Figure 18: Distribution of black holes in the plane M_{BH}/M_{\odot} versus spin a^* .

If we take into account the presence of an axion [14] there will be a cloud of axions exponentially growing in each l-zone, this will make the black hole lose spin until leaving the superradiance region. Thus in the presence of axions we expect no BHs in the regions where superradiance occurs. After a certain time, the distribution for 10,000 black holes will be like this:

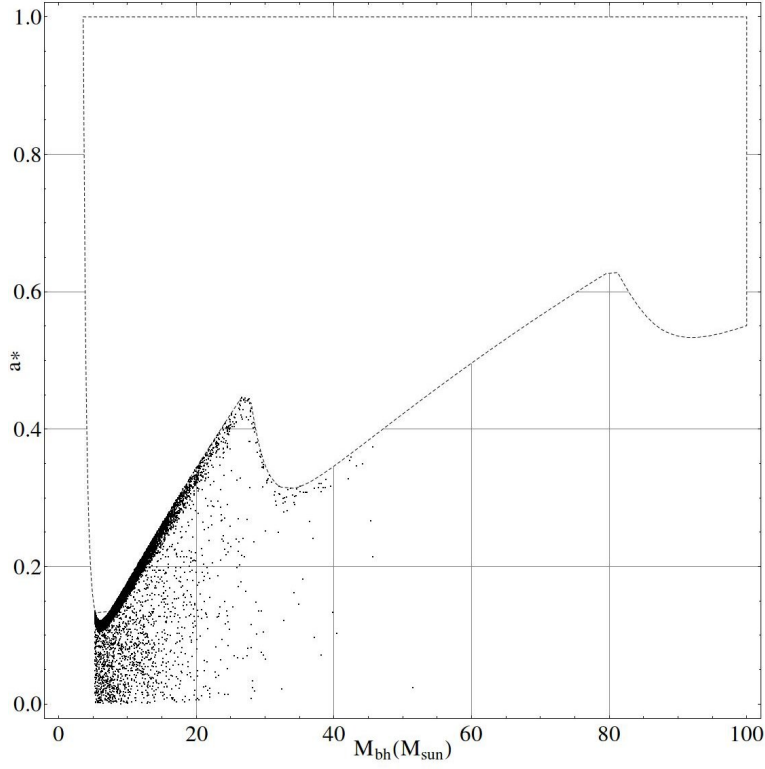


Figure 19: Distribution of black holes with an axion of $\mu_a = 6 \cdot 10^{-13}$ eV.

We see that all the BHs initially located in the superradiance regions have moved down into a region where superradiance is no longer valid. This shows that axions through the effect of superradiance can have a measurable effect on the BH distribution. By measuring mass and spin of a large amount of BHs, the existence of axions could be proven, in principle. According to [14], it is much more complicated to measure this effect in an experiment, due to large errors in the measurement of the BH spin.

6 Conclusions

In this report we have discussed the Hierarchy problem and investigated one of its possible solutions, the Relaxion models. We have seen that dynamical models like the original and the double scanner model could in principle result in a value for the Higgs vev: $v \ll M_{\text{new physics}}$. This value would be naturally small and would thus not suffer from fine-tuning. However, there are a large number of conditions which have to be fulfilled by these axions.

We have investigated the Relaxation models by simulating the dynamics using Mathematica and have tested the effect the different parameters/constants have on the dynamics.

These models require the existence of light axions. The hope is to find these axions in the future by looking, for example, at the BH distribution and distinguish the effect of superradiance from the axion cloud on this distribution.

7 Acknowledgements

We would like to thank Christophe Grojean for his guidance and proofreading of this report. Moreover, we are also grateful to DESY and the Theory Group, who have welcomed us within the Summer Student Programme. All Feynman graphs were drawn using the Jaxodraw, and for the plots and simulations we used Wolfram Mathematica 9.0.

References

- [1] F. Brümmer, “Lecture notes on Beyond the Standard Model Physics, given at the DESY Summer Student Programme.” <https://summerstudents.desy.de/hamburg/e224192/e225266/Beyond-the-Standard-Model-1.pdf>, August, 2016.
- [2] G. ’t Hooft, “Naturalness, chiral symmetry, and spontaneous chiral symmetry breaking,” *NATO Sci. Ser. B* **59** (1980) 135.
- [3] P. W. Graham, D. E. Kaplan, and S. Rajendran, “Cosmological Relaxation of the Electroweak Scale,” *Phys. Rev. Lett.* **115** no. 22, (2015) 221801, [arXiv:1504.07551 \[hep-ph\]](#).
- [4] J. R. Espinosa, C. Grojean, G. Panico, A. Pomarol, O. Pujolàs, and G. Servant, “Cosmological Higgs-Axion Interplay for a Naturally Small Electroweak Scale,” *Phys. Rev. Lett.* **115** no. 25, (2015) 251803, [arXiv:1506.09217 \[hep-ph\]](#).
- [5] R. D. Peccei and H. R. Quinn, “Constraints Imposed by CP Conservation in the Presence of Instantons,” *Phys. Rev.* **D16** (1977) 1791–1797.
- [6] H. Baer, K.-Y. Choi, J. E. Kim, and L. Roszkowski, “Dark matter production in the early Universe: beyond the thermal WIMP paradigm,” *Phys. Rept.* **555** (2015) 1–60, [arXiv:1407.0017 \[hep-ph\]](#).
- [7] “Any light particle search.” <https://alps.desy.de/>. Accessed: 2010-09-04.
- [8] A. Arvanitaki, M. Baryakhtar, and X. Huang, “Discovering the QCD Axion with Black Holes and Gravitational Waves,” *Phys. Rev.* **D91** no. 8, (2015) 084011, [arXiv:1411.2263 \[hep-ph\]](#).
- [9] V. Lahu, “Dynamics of the weak scale Relaxation,” Master’s thesis, École Polytechnique de Lausanne, Switzerland, Not yet finished.
- [10] C. W. Misner, K. S. Thorne, and J. A. Wheeler, *Gravitation*. Macmillan, 1973.
- [11] M. Guidry, “Rotating black holes.” http://eagle.phys.utk.edu/guidry/astro490/lectures/lecture490_ch13.pdf. Accessed: 2010-09-04.
- [12] A. Arvanitaki and S. Dubovsky, “Exploring the String Axiverse with Precision Black Hole Physics,” *Phys. Rev.* **D83** (2011) 044026, [arXiv:1004.3558 \[hep-th\]](#).
- [13] W. M. Farr, N. Sravan, A. Cantrell, L. Kreidberg, C. D. Bailyn, I. Mandel, and V. Kalogera, “The Mass Distribution of Stellar-Mass Black Holes,” *Astrophys. J.* **741** (2011) 103, [arXiv:1011.1459 \[astro-ph.GA\]](#).
- [14] A. Arvanitaki, M. Baryakhtar, S. Dimopoulos, S. Dubovsky, and R. Lasenby, “Black Hole Mergers and the QCD Axion at Advanced LIGO,” [arXiv:1604.03958 \[hep-ph\]](#).